Scientific Research Publishing

American Journal of Analytical Chemistry, 2022, 13, 135-161
https://www.scirp.org/journal/ajac
ISSN Online: 2156-8278
ISSN Print: 2156-8251

Microwave Detection, Disruption, and Inactivation of Microorganisms

Victor J. Law*, Denis P. Dowling

School of Mechanical and Materials Engineering, University College Dublin, Dublin, Ireland
Email: *viclaw66@gmail.com

How to cite this paper: Law, V.J. and Dowling, D.P. (2022) Microwave Detection, Disruption, and Inactivation of Microorganisms. *American Journal of Analytical Chemistry*, **13**, 135-161.
https://doi.org/10.4236/ajac.2022.134010

Received: February 28, 2022
Accepted: April 18, 2022
Published: April 21, 2022

Abstract

This paper reviews three complex interactions between microwave energy and microorganisms (bacteria, fungi, and viruses). The first interaction comprises the detection of viruses within human blood using a 50-Ohm transmission-line vector net-analyzer (typically 0 to 10 dBm @ 2 to 8.5 GHz) where the blood is placed within a test chamber that acts as a non-50-Ohm discontinuity. The second interaction employs 1 to 6.5 W @ 8 to 26 GHz for microwave feed-horn illumination to inactivate microorganisms at an applied power density of 10 to 100 mW^{-2}. The third interaction is within multi-mode microwave ovens, where microorganism cell membrane disruption occurs at a few 100 s of W @ 2.45 GHz and microorganism inactivation between 300 to 1800 W @ 2.45 GHz. Within the first microwave interaction, blood relaxation processes are examined. Whereas in the latter two microwave interactions, the following disruption, and inactivation mechanisms are examined: chemical cellular lysis and, microwave resonant absorption causing cell wall rupture, and thermodynamic analysis in terms of process energy budget and suspension energy density. In addition, oven-specific parameters are discussed.

Keywords

Bacteria, Fungi Virus, Hepatitis C Virus, Human Immunodeficiency Virus, Detection, Disruption Inactivation, N95 Respirator, Microwave Oven

1. Introduction

The scientific origins of vaccination and thermal inactivation of bacteria, fungi, and viruses go back to the pioneering work of Edward Jenner (1749-1823) and Louis Pasteur (1822-1895). By 1900, Herbert George Wells brought the idea of beneficial and pathogenic microorganisms to the forefront in his novels "*The*

Time Machine" [1] and the "*War of the Worlds*" [2]. The latter manifested itself in the 1918-1920 influenza pandemic which was caused by the H1N1 virus [3]. Since 2009, the world has undergone two further major influenza pandemics (caused by the subtype of the H1N1 [4]), and the SARS-CoV-2 virus [5]. In the latter pandemic, wealth and political pressure have generated a global disparity in vaccine uptake between nations, leading to travel restrictions between world regions [6]. In addition, single-use personal protective equipment (such as surgical masks and N95-like respirators) has become an environmental waste problem [7]. Due to the rapid spread of the Omicron variant some two years into the COVID-19 pandemic, some nations (Greece, Christmas—New Year, 2021) have introduced the compulsory wearing of N95-like respirators by the general public. Arguably, the N95 particle filtering standards have brought to the limelight within the public perception of the transmissibility of influenza viruses that have a spheroid diameter of 80 to 300 nm.

This paper reviews a range of potential interactions between microwave energy and microorganisms. For example, there are a number of microwave-based technologies in the development of *in-vitro* rapid detection of coronavirus (COVID-19) within human blood [8] [9] [10] [11]. These use mono-mode 50-Ohm transmission-line applicators, plus *in-vivo* inactivation of COVID-19 of an infected individual [12]. For *in-vitro*, single batch multi-mode microwave oven inactivation of bacteria, fungi, and influenza virus [13] [14] [15] [16] [17], cell membrane disruption [16] [18], sterilization of towels [17], inactivation of Hepatitis C Virus (HCV), Human Immunodeficiency Virus (HIV) inoculated syringe, cigarette filters [19], continuous flow inactivation of airborne and liquid-borne microorganisms within modified microwave ovens have been reported [20] [21] [22]. In the latter [22], the calorimetric calculation method was used to estimate the energy required to inactivate bacteria in both airborne and water-borne phases. Microwave Generation Steam (MGS) decontamination of virus inoculated N95-like respirators within domestic and industrial multi-mode microwave ovens has also been reported [23]-[28], along with thermodynamic analysis and dielectric considerations of MGS have been explored [29] [30]. Mono-mode microwave feed-horn inactivation of influenza virus has been examined [31] [32] [33] [34] [35].

Microwave applicators may be classified into two types: mono-mode (or single-mode) and multi-mode. The microwave oven is a well-known example of a multi-mode applicator in which a complex electromagnetic field pattern is formed by the superimposition of different electromagnetic waves and multiple cavity wall reflections [36] [37] [38]. Consequently, with sufficient energy, dielectric volume heating of organic material (food stuff, or culture fluid containing microorganisms) may undergo non-uniform heating due to size, geometry, and location within the oven's multi-mode cavity [29] [30]. Mono-mode applicators, such as a 50-Ohm transmission line produce coherent standing waves on the line, where the Standing Wave Ratio (SWR) is determined by the line impedance load termination. Indeed, open-ended transmission lines are used to measure the dielectric properties of polar molecules such as water [39].

This paper is constructed as follows. Section 2 examines *in-vitro* rapid detection of influenza virus within human blood. Section 3 looks at the inactivation of influenza viruses by mono-mode microwave feed-horn applicators. Section 4 examines multi-mode microwave ovens technology reported for the inactivation and disruption of bacteria, fungi, influenza virus, HCV and HIV. In this work, the term gram-negative and gram-positive (originally used by Hans Christian Gram (1853 to 1938) who developed specific dyes to differentiate microorganisms when viewed under a microscope) is used to differentiate microorganisms that have different membranes or wall structures. Gram-negative microorganisms have an outer membrane (*Escherichia coli* (*E. coli*) *Pseudomonas aeruginosa* (*P. aeruginosa*) and *Pseudomonas fluorescens* (*P. fluorescens*)), while gram-positive microorganisms (*Bacillus subtilis* var niger (*B. subtilis* var niger), *Candida albicans* (*C. albicans*) and *Staphylococcus aureus* (*S. aureus*)) have no outer membrane. Section 5 looks at MGS decontamination of virus inoculated N95-like respirators. Section 6 provides a discussion on the reviewed papers, Section 6.1: virus rapid detection methods, Section 6.2: mono-mode feed-horn inactivation of microorganism and mechanisms of destruction, Section 6.3: microorganism sample size, geometry, and location within microwave oven, Section 6.4: respirator metal nose clips, Section 6.5: bubble formation and Section 6.6: non-thermal and thermal microwave oven inactivation mechanism. Section 7 provides a summary and outlook of this work. *In-Vivo* inactivation of COVID-19 of an infected individual [12] is not considered in this work.

2. *In-Vitro* Rapid Detection of Influenza Virus within Human Blood

It is well known that normal (healthy) human blood is an amalgamation of approximately 55% plasma and 45% blood cells (erythrocytes and leukocytes and thrombocytes). These blood cells are typically 10 to 50 time's size of influenza viruses. Since the early 1950s [40] [41] microwave (1.7 to 24 GHz) measurements have shown that the dielectric constant (ε_r¢) of human blood exhibits an inverse frequency dependency. Within this dependency there are at least two flat (relaxation) regions: β-dispersion arising from the polarization of the cell membranes in the 10 kHz to 200 MHz region and the γ-dispersion region (near 18 GHz) due to the reorientation of water molecules [42]. Glucose [43] [44] [45] and anticoagulant agents [46] are also known to alter the dispersion which has a significant importance in biosensor diagnostics. In addition, the dispersion is known to be gender specific [46]. Unlike most bacterial and virus infections that cause an increase in leukocyte and lymphocyte count, recent studies of influenza virus infections found a increase in leukocyte lymphocytes count [47] [48]. Given this knowledge *in vitro* studies into human blood (with and without coronavirus) within a 50-Ohm transmission-line that incorporates a blood sample test chamber have been undertaken using a Vector Network Analyzer (VNA). In this configuration, the test chamber plus blood acts as a variable non 50-Ohm discontinuity [49] [50]. Examples of the use of both contact and non contact antenna mea-

surements [8] [9] are summarized below.

Figure 1(a) shows a schematic of a bench-top Agilent 2-port PNA-L (VNA) scattering parameter (S-parameter, where S_{12} is transmission and S_{11} is reflection) measurement of human blood [8]. **Figure 1(b)** shows a typical S_{11} swept frequency response, with no blood added (control; solid line) to a planer circular ring, healthy blood (dotted line) and COVID-19 blood (dashed line). A feature of note is that when healthy blood is in contact, the primary S_{11} zero frequency registration reduces from 4.7 to 4.38 GHz with respect to the control. When a COVID-19 blood sample is in contact, the primary zero shifts to 5.1 GHz which equals to a positive frequency shift of 720 MHz with respect to healthy. In addition, the apex of the shifted S_{11} zero falls approximately from −12 to −15 dB, with respect to the healthy blood zero. The secondly S_{11} zero (not shown here) is in the region of 6.5 GHz forms the beginning of a ripple that is related to the transmission-line length, see Equation (1) [49] [50].

$$\Delta f = \frac{cV_p n}{2l} \tag{1}$$

where c is the velocity of light (2.997×10^8 m/s), V_p is the inverse square root of the transmission-line dielectric constant: for a polyethylene transmission-line V_p = 0.65 to 0.67. The symbol n is the integer number of ripples in a given sweep

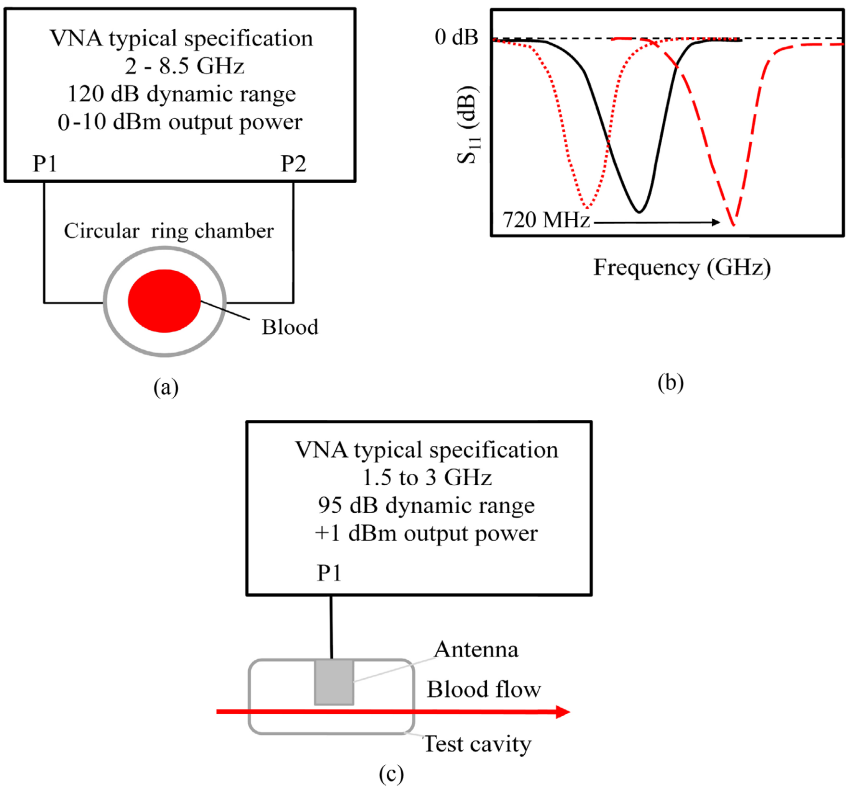

Figure 1. (a) VNA 2-port transmission and reflection, (b) S_{11} swept frequency analysis of circular ring chamber (control; solid line), healthy blood (dotted line), and COVID-19 blood (dashed line). (c) Portable 1-port VNA and non-contact antenna measurement (S_{11} and S_{11} phase) of COVID-19.

range and l is the transmission-line length. With c and 2 being constant, the ratio of V_p/l enables the reflection plane to be identified and followed, particularly at the zero that is closest to the blood resonant frequency where the greatest signal response is obtained.

In 2021, Elsheakh *et al.* [9] reported on a portable/handheld Agilent N9918A 1-port VNA S_{11} measurement of continuous flowing human blood which is passed over a microwave resonating planar microstrip antenna. In this case the antenna does not come into direct contact with the blood, and the VNA has less dynamic range and available output power compared to the Agilent PNA-L VNA [8]. **Figure 1(c)** shows a schematic of the microwave set-up. In this arrangement both healthy blood and blood containing COVID-19 are sequentially passed over the antenna (resonating in the 2.45 GHz industrial, scientific and medical (ISM) frequency band), both of which are placed within a chamber. As a control, S-parameter (S_{11} and S_{11} phase), measurements are taken without blood flow, then with healthy human blood flow, and COVID-19 contaminated human blood flow. In these three measurements the length of the transmission-line between the VNA and antenna induces a ripple in the frequency response according to the test chamber impedance [49] [50]. At present, logistic regression analysis of theses measurement have yielded a binary outcome (positive or negative COVID-19). Using 66 samples the authors claim a COVID-19 detection accuracy of 63.3% for S_{11} and 60.6% for S_{11} phase measurements both of which compare favorably with current molecular polymerase chain reaction tests.

3. Inactivation of Influenza Viruses by Mono-Mode Microwave Feed-Horn Applicator

Inactivation of microorganism using mono-mode microwave feed-horn irradiation has been reported by a number of research groups [31] [32] [33] [34] including a US Patent [35]. Generally the microwave feed-horn applicator comprises a frequency source, amplifier, and feed-horn that illuminate the virus suspension. However there are three means of energy illumination. **Figures 2(a)-(c)** shows three such means of illumination: direct broadband swept frequency illumination [35] **Figures 2(a)**, direct narrowband frequency illumination **Figures 2(b)**, and parallel reflectarray and focusing reflectarray **Figures 2(c)**. In the case of **Figure 2(b)** and **Figure 2(c)** [31] [33] it has been established that the optimum operating frequency for influenza virus inactivation is in the frequency range of f_0 = 8.0 to 8.5 GHz. Examples of virus inactivation by microwave feed-horn illumination by Hung *et al.* and [32] and Yang *et al.* [33] are given in Section 3.1.

Virus Inactivation by Microwave Feed-Horn Illumination

In 2014, Hung *et al.* [32] has used a microwave focusing reflect array (**Figure 2(c)**) operating at a power of 1 W continuous wave (CW) at 8 GHz to inactivate influenza virus subtype H3N2. The virus was immersed in a culture fluid suspension within a 10 cm^2 flat Petri dish with a focal point distance of 178 mm from

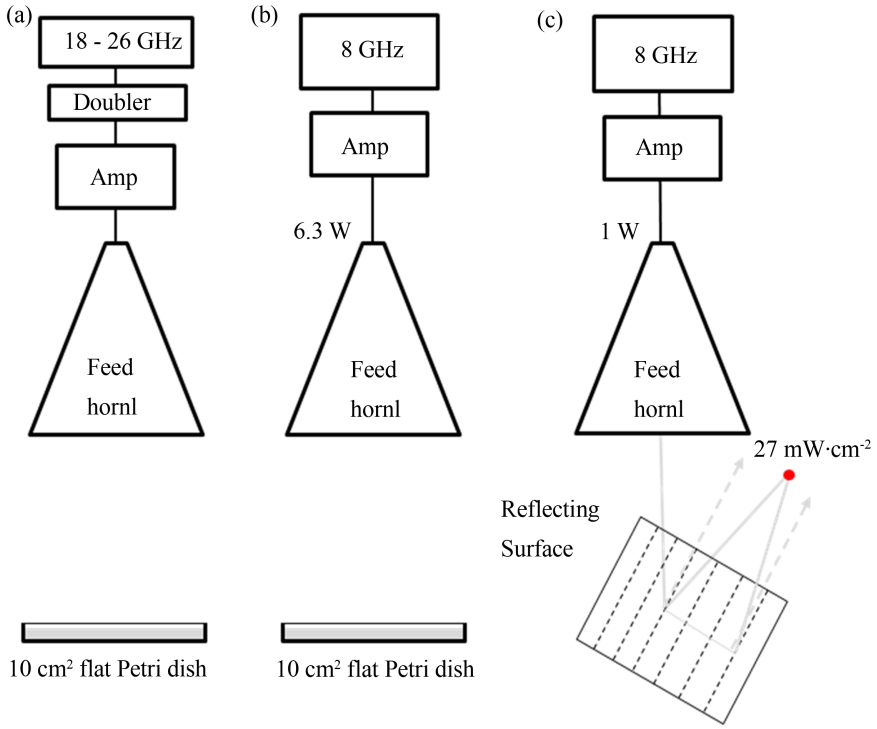

Figure 2. (a)-(c) Three examples of microwave feed-horn used for illmination of virus. (a) Direct broadband swept frequency illumination [35], (b) direct narrowband frequency illumination [32], and parralel reflect array, and fousing array illumination [33] (c).

the focusing array. Their findings revealed, that for a 15 minute irradiation exposure time with a power density of 27 mW·cm^{-2} that an inactivation efficiency of 93 % was achieved within the focal area could be obtained.

Yang *et al.* 2015 [33] used direct microwave illumination (**Figure 2(a)**) to inactivate influenza virus subtype H3N2 in the 8.0 to 8.4 GHz range. The input power to the feed-horn was 3.6 W CW at 8.4 GHz. For a similar exposure time of 15 minutes to that of Hung [32], a calculated average illumination power density of 81 mW·cm^{-2} was found to produce a subtype H1N1 and H3N2 suspension inactivation efficiency in the region 90% to 100%.

4. Inactivation of Bacteria and Virus within Domestic Multi-Mode Microwave Ovens

This section outlines how multi-mode domestic microwave oven can be used for the thermal and non-thermal inactivation studies of homogeneous microorganism populations. In each case the microwave power source employs a free-running cavity-magnetron frequency is $f_0 = 2.45 \pm 0.1$ GHz. Normally the magnetron manufactures stated power, is calibrated using the open water bath method, where the temperature rise of water (1000 ml) is measured over time for a given power level setting [29] [30] [51] [52] [53], based on Equation (2).

$$P = mC\frac{\Delta T}{t} \tag{2}$$

where P is power (W, or $J \cdot s^{-1}$), m is the mass (g) of water, C is heat capacity (4.184 $J \cdot g^{-1} \cdot K^{-1}$) of water, ΔT is the change in water temperature (final temperature minus the initial temperature), and t is the heating time measured in seconds. Given this method of power calibration for a domestic microwave oven, at full power the cavity-magnetron operates in the CW mode, or duty-cycle (D) = 100%. For power settings below full power, the cavity-magnetron is sequentially pulsed on and off. For example, a power setting that employs D = 50%, the on-period (t_{on}) is equal to the off-period (t_{off}). Thus for the t_{on} period, the microorganism suspension undergoes dielectric volume heating, and in t_{off} the microorganism suspension cools under conduction processes throughout the suspension volume. For the purpose of this work, the terms: non-thermal microwave and thermal microwave inactivation are used. **Figure 3** shows the first series of t_{on} and t_{off} pulses, with the suspension not cooling to its initial temperature. Under these conditions the suspension experiences a step-like incremental increase in temperature over time [53] [54].

The study of microorganism membrane disruption normally requires sublethal conditions, the technique of non-thermal [16] (or, athermal [18]) microwave irradiation has between developed for this purpose, where the aim is to remove, or lower, the induced thermal heat thereby attempting to isolate the microwave irradiation effect (**Figure 3**). This is achieved by cooling (26˚C - 29˚C [16] [18]) the vessel containing the microorganism suspension in the microwave oven and using a D < 100%. For air forced cooling of organic compounds see [55] [56] [57]. The thermal heat is thus removed at the containing vessel wall and by conduction thought out the suspension in the t_{off} period. In practice, most domestic microwave oven control circuits have a t_{off} period limited to 15 to 30 seconds to protect the cavity-magnetron's cathode [52]. This may lead to a situation where a selected minute process time at medium to low power results in $T_{on} = T_{off}$ which equates to 30 seconds of microwave irradiation and 30 seconds no irradiation.

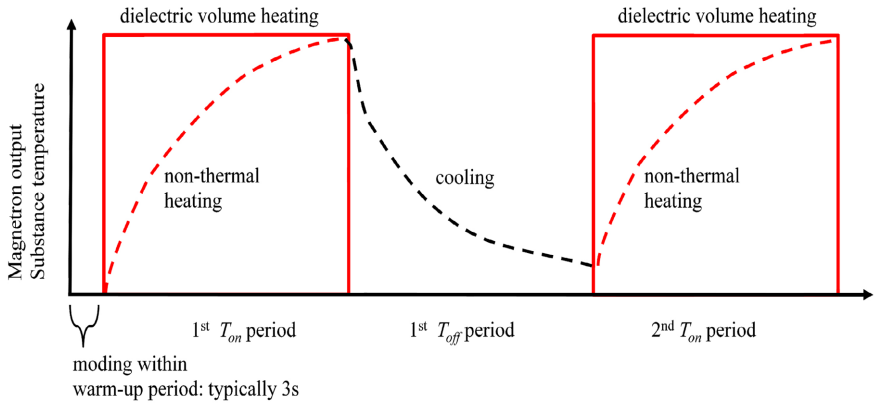

Figure 3. Schematic of thermal and non-thermal microwave heating within a domestic microwave oven. Thermal microwave dielectric volume heating (solid line) and non-thermal dashed line.

4.1. Multi-Mode Microwave Oven Batch Processing of Microorganisms

This section describes single batch *in-vitro* processing of microorganisms. The vessels considered here are: beaker, flat Petri dish, kitchen pads, syringe towels, and N95-like respirators. Figure 4(a) and Figure 4(b) shows the location of beaker, flat Petre dish, and syringe within a microwave oven. Depending upon the reference paper (13 - 19, 23 - 28) the inactivation is given either as a Log_{10} reduction ($\text{Log}_{10}(A/B)$, or percentage reduction ($A - B * 100/A$) as a function of experiment conditions. Where the inactivation is reported as total, an equivalent log reduction of 7 is given [58].

4.2. Multi-Mode Microwave Oven Batch Treatment of *E. Coli*

In 1992, Fujikawa *et al.* [13] studied the inactivation kinetics of a gram-negative *E. coli* suspension within a RE-S650 - Sharp Corporation microwave oven. The study was performed as function suspension geometry (cylindrical beaker (200 ml) or flat Petri dish (109 mm diameter × 17 mm high), phosphate buffer and pH suspension, exposure time (0 to 4 minutes), a fixed rated power level of 100, 200, 300 W with sample placed on a 2.46 rpm glass rotating carousel (Figure 3(a) and Figure 3(b)). They found for each unit volume of bacterial suspension, the temperature (T) and bacterial survival rate after a given microwave exposure are a functions of suspension pH, suspension, location, geometry (beaker of flat Petri dish), and exposure time (see Table 1).

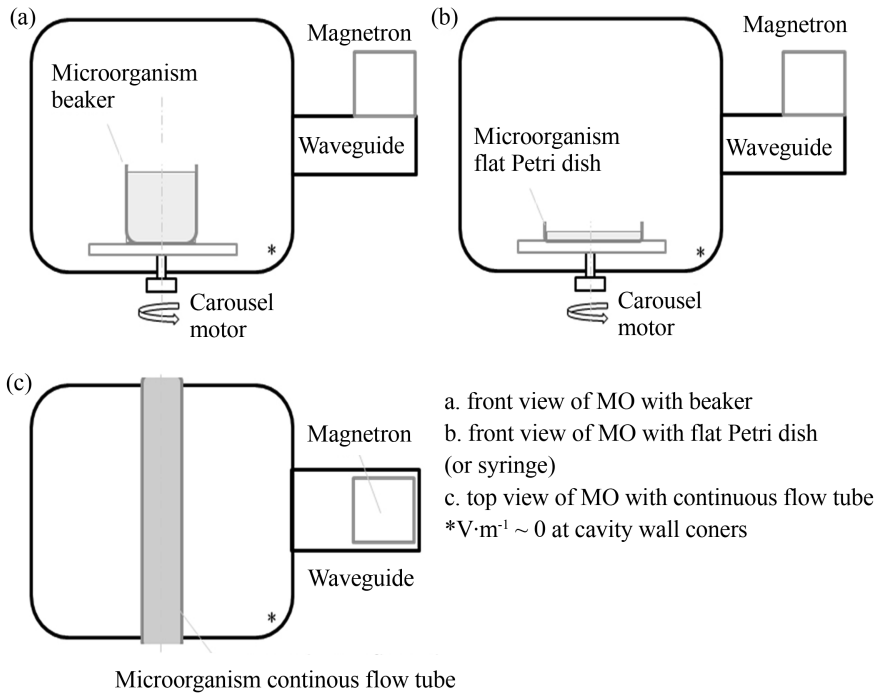

Figure 4. (a)-(c) Cartoon of multi-mode microwave ovens for inactivation of microorganism. (a) Batch location of microorganism: beaker [13] [14] [18], (b) flat Petri dish [16], syringe [15] [19] towels [17], and (c) continuous flow tube [20] [21] [22].

Table 1. Multi-mode microwave thermal inactivation of gram-negative *E. coli* [13] [14] [15] [16].

Reference	Beaker, flat Petri dish, syringe	Thermal (˚C) Non-thermal (˚C)	Power (W)	Exposure time (s)	Inactivation (Log_{10} reduction)
[13]	Beaker 200 ml	Thermal (~60˚C)	100	240	~5log_{10}
	Beaker 200 ml	Thermal (~60˚C)	200	150	~4log_{10}
	Beaker 200 ml	Thermal (~65˚C)	300	90	~6log_{10}
	Beaker 200 ml	Thermal (~60˚C)	200	150	~4log_{10}
	Flat Petri dish	Thermal (~40˚C)	200	90	Non change
[14]	Beaker 500 ml	Thermal (~70˚C)	600	60	~5log_{10}*
[15]	Sponge (7.37 cm^3; 6.43 ml water)	Thermal (~92˚C inside, 80˚C surface)	1050	60	~7log_{10}
	Scrubbing pad (41.62 cm^3; 10.94 ml water)	Thermal (~84˚C surface)	1050	120	~4log_{10}
	Used 10 ml plastic syringe	Thermal (~80˚C surface)	1050	240	~7log_{10}
[16]	Flat Petri dish	Thermal (~52˚C)	650	20	~1log_{10}
	Flat Petri dish	Thermal (~70˚C)	650	40	~7log_{10}*

*Leakage of nucleic acid in suppression, cell membrane disruption via puncturing of the cell membrane.

Woo, Rhee and Park 2000 [14] used a MR301M-LG Electronics, Inc., microwave oven for inactivation of *E. coli* and *B. subtilis* suspensions. After each microwave thermal inactivation experiment they measured the nuclei acid within the suspension and imaged the bacteria outer surface using a Scanning Electron Microscope (SEM) and Transmission Election Microscope (TEM). The *E. coli* suspension temperature and inactivation data is given in **Table 1**.

Later in 2006, Park *et al.* [15] studied inactivation of *E. coli* inoculated kitchen sponge (3.17 × 3.37 × 0.69 cm), kitchen non-metallic scrubbing pad (9.06 × 7.07 × 0.65 cm), and 10 ml-plastic syringe within a RE-S630D0 - Sharp Corporation microwave oven (**Figure 3(a)** and **Figure 3(b)**). The material of the sponge foam and scouring pads are not given, but given related patent information at the time the martial used is most likely to be open-cell polyurethane foam and non-woven nylon, respectively [59]. The inactivation was performed as a function time at a fixed cavity-magnetron rated power of 1 or 1.1 kW (reported here as 1050 ± 0.050

W). In addition, thermal temperature measurements were performed to estimate the *E. coli* suspension temperature throughout each inactivation experiment. Their results are given in Table 1.

Asay *et al.* 2008 [16] studied thermal and non-thermal (26˚C ± 1˚C) microwave inactivation of 10 ml *E. coli* suspension within a flat Petri dish, placed on a rotating glass carousel within a ER-754BTC Toshiba microwave oven (Figure 3(b)). The power was set to # 5 out of 9 levels, where 9 is maximum cavity-magnetron rated power of 650 W). The temperature and inactivation as a function of both power and time are shown in Table 1. In addition, propidium iodide staining (the uptake is inversely correlated with cell viability due to loss of membrane integrity) and β-galactosidase assay (an indicator of thermal protein denaturation) were performed. The thermal microwave inactivation results are shown in Table 1, while the non-thermal results are given in Table 2.

In 1998, Tanaka *et al.* reported on microwave oven sterilization of moist towels that where inoculated using (1 ml aliquots on 7 × 7 cm gauze) of *S. aureus*, *P. aeruginosa* and *C. albicans*. The microwave oven (Corona Co., Ltd., Tokyo) [17] had a rated microwave power of 500 W and irradiation time of 1 minute for a single moist towel and 2 minutes for three moist towels. Section 6 gives further information on this study.

In 2006, Benett *et al.* [18] reported on microwave non-thermal disruption of *E. coli* suspension within a 50 ml beaker that was cooled by an ice bath (20˚C to 29˚C) when microwave irradiated within a Panasonic microwave oven (Mn-5853C; rated cavity-magnetron power = 800 W). Microwave irradiation exposure was performed at a medium-low power setting for: 15, 20, 25, 30, 35, and 40 s. After exposure, propidium iodide staining was performed to investigate membrane integrity. Colonies where also counted for cell viability. The sample temperature and disruption data is given in Table 2. Their viability experiment revealed a decrease in viable cell count from ~9.8×10^8 at 15 s; ~9×10^8 at 20 and; 6.4×10^8 cell ml^{-1} at 25 s. This was followed by a leveling-off cell count in the 30, 35, and 40 s exposure times with a mean value of ~$5.3 \pm 0.5 \times 10^8$ cell ml^{-1}.

In 2016, Siddharta *et al.* [19] reported upon the microwave oven inactivation of HCV and HIV contaminated syringes and cigarette filter papers with the aim

Table 2. Multi-mode microwave non-thermal membrane disruption of gram-negative *E. coli* [16] [18].

Reference	Beaker, flat Petri dish	Non-thermal (˚C)	Power (W)	Exposure time (s)	Stain observation
[16]	Flat Petri dish	Non-thermal (26˚C ± 1˚C)	650	20 - 40	Outer membrane disruption
[18]	Beaker 50 ml, cooled in 500 ml crushed ice bath	Non-thermal (20˚C - 29˚C)	Medium to low power	25*	Outer membrane disruption

* Exposure time where cell viability count leveled-off.

to mimic re-use within a population of People Who Inject Drugs (PWID). A Bosch microwave oven (type: MM817ASM, cavity-magnetron rated power of 800 W) was used for this purpose, along with insulin syringes (40 ml, with needle removed), and slim cigarette filters (6 × 15 mm). For the syringe, a HCV and/or HIV suspension is used to spike the syringe. While to mimic storage of used cigarette filters, the virus suspension was allowed to be soaked-up (approximately 0.5 ml [60]) by the filter and then dried in household foil. **Table 3** provides the temperature and inactivation data for an irradiation time of 3 minutes at 90, 180 and 360 W for contaminated syringe and cigarette filter papers.

4.3. Microwave Oven Continues Flow Gram-Positive and Gram-Negative Microorganism Inactivation

In 2010, Wu and Yao [20] reported on a modified microwave oven continuous flow inactivation process for bacteria (gram-positive *B. subtilis* var niger and gram-negative *P. fluorescens*) and mold fungi (gram-positive *A. versicolor*). A commercial microwave oven (Midea Inc, Foshan, Guangdong Province, China) was used for this purpose (**Figure 4(c)**). This works reports the magnetron operating power conditions: full CW power = 700 W (100% duty cycle (30 s in 30 s), duty cycle 12 s in 30 s for medium power (384 W), and duty cycle 5.1 s in 30 s at the low power setting (119 W). Both airborne and liquid-borne microorganism suspensions were microwave irradiated at pre-set microwave power levels of 119, 384 and 700 W for exposure times between 1 and 3 minutes. **Table 4**, gives the microorganism inactivation (survival rate) as a function experiment conditions. Both SEM and TEM imaging were performed on the microorganisms after microwave irradiation.

Further in 2014, Wu and Yao [21], reported on airborne and liquid-borne survival rate/inactivation of MS2 bacteriophage (a surrogate for the 2009 pandemic H1N1 influenza virus) using the same modified microwave oven (**Figure 2(c)**) and power level setting as reported in [20]. The aerosol oven exposure times used were: 1.7, 2, 3, and 5 minutes. **Table 5** gives the microorganism inactivation

Table 3. Multi-mode microwave thermal decontamination of HCV and HIV spiked insulin syringe and cigarette filter [19].

Virus 3 minute exposure time	Inactivation		
	90 W	180 W	360 W
Insulin syringe—HCV	No change (~33˚C)	No change (~52˚C)	~4 $\log_{10}$ (~70˚C)
Insulin syringe—HIV	No change (~33˚C)	No change (~52˚C)	~4 $\log_{10}$ (~70˚C)
Dried cigarette filter—HCV	No change (~33˚C)	No change (~52˚C)	~4 $\log_{10}$ (~70˚C)
Dried cigarette filter—HIV	No change (~33˚C)	No change (~52˚C)	~4 $\log_{10}$ (~70˚C)

Table 4. Multi-mode microwave thermal inactivation of gram-positive and negative microorganisms under continuous flow conditions [20].

Microorganism (exposure time)	Inactivation (survival rate)		
	119 W	384 W	700 W
Airborne (1.5 minutes)			
B. subtilis var niger	35%	44%	35%
P. fluorescens	21%	12%	6%
A. versicolor	25%	20%	11%
Liquid-borne			
B. subtilis var niger (1 minutes)	100%	35%	28%*
B. subtilis var niger (2 minutes)	100%	22%	4%*
B. subtilis var niger (3 minutes)	46%	25%	0%*
P. fluorescens (1.5 minutes)	0%	0%	0%*
A. versicolor (1.5 minutes)	0%	0%	0%*

The gray text denotes that *P. fluorescens* is classified as gram-negative bacteria. *SEM and TEM images showed visible damages to the microwave-irradiated liquid-borne.

Table 5. Multi-mode microwave thermal inactivation of MS2 bacteriophage under continuous flow conditions [21].

Microorganism	Inactivation (average survival rate)		
	119 W	384 W	700 W
Airborne			
MS2 (resident time 1.7 minutes)	~50%	~35%	~10%*
Liquid-borne			
MS2 (2 minutes)	~74%	~44%	~6%*
MS2 (3 minutes)	~44%	~17%	~4%*
MS2 (5 minutes)	~18%	~6%	~5%*

*SEM and TEM images showed visible damage to MS2 bacteriophage.

(survival rate) as a function experiment conditions. Scanning electron microscope and TEM imaging of 700 W irradiated microorganisms highlighted the presence of visible damage to both cell membrane and elements within the cytoplasm.

In 2019, Wang *et al.* [22], reported on continuous flow airborne and liquid-borne inactivation of gram-negative *E. coli*. The continuous flow tube having a 100 mm diameter, 1 mm wall thickness positioned within a microwave oven (M1-L213B, China), **Figure 2(c)**. The microorganisms were irradiated at a microwave power level of 700 W between with flow adjusted to produces exposure times between 0 and 20 minutes. **Table 6** gives the *E. coli* inactivation as a function

Table 6. Multi-mode microwave thermal inactivation of gram-negative *E coli* continuous flow (airborne and liquid-borne [22].

Microorganism 20 s and 5 minutes exposure time	Inactivation (700 W)
Airborne *E. coli* (20 s)	2.6 $\log_{10}$ (22˚C)
Airborne *E. coli* (5 minutes)	Total (40˚C)
Liquid-borne *E. coli* (20 s)	0.6 $\log_{10}$ (~22˚C)
Liquid-borne *E. coli* (5 minutes)	2.45 $\log_{10}$ (~75˚C)

of airborne and liquid-borne microwave power and exposure time. In their analysis they used the calorimetric calculation (Equation (3)) to measure the heat involved in raising the temperature of air and water.

$$Q = mC\Delta T \tag{3}$$

where Q is the specific heat (J), m is the mass (g) of the substance, C is heat capacity ($J \cdot g^{-1} \cdot K^{-1}$) of the substance, and ΔT is the temperature change of the substance.

5. MGS Decontamination of Virus Inoculated N95-Like Respirators

In a response to the 2009 and 2019 influenza virus pandemics, experimental studies in to MGS decontamination of bacteria and influenza virus inoculated N95-like respirators have been reported [23]-[28]. The aim of these studies was to kill the microorganisms whilst keeping the physical and visual properties of the respirators intact with a view to re-use the respirators. Like the decontamination of HCV and HIV inoculated syringes and cigarette filters [19] there is a temperature limited processing widow for N95-like respirators. Below 70˚C it is found that there is insufficient: virus inactivation, whereas at the boiling point of water (100˚C) and prolonged irradiation times there is a loss of respirator filter void, loft, structural failure at respirator component interface, plus metal noise clip burning. To improve the understanding of the MGS decontamination process window, a thermodynamic analysis of the process along with dielectric considerations have been reported [29] [30].

As detailed in **Table 7**, the thermodynamic analysis can be carried out using Equations (2) and (3) to estimate the energy input and energy output (Q), and liquid-phase water conversion into steam for six bacteria and virus inoculated N95-like respirators studies. It was found that many of the experimental variables (rated and applied power) were not reported sufficiently; data mining of supporting research papers and commercial information was undertaken. With this approach, an estimation of the process energy budget and its pathway between raising temperature of the liquid-phase water and the production of steam was made for each microwave oven. The analysis of N95-like respirators outcome with the associated process energy input also allowed meaningful

Table 7. Multi-mode thermal MGS decontamination of inoculated N95-like respirators.

Microorganism	Energy input calculations			Energy output calculations			
	Power (W)	Energy (kJ)	Water (g)	Temperature change (DT)	Q (kJ)	Energy steam conversion (kJ)	Liquid (g), steam (L)
Bergman [23]	750	90	100	80	33.5	56.5	*25* *41.7*
H1N1 influenza virus [24]	1250	150	100	76.5	32	118	52.2 87.2
MS2 bacteriophage [25]	750	65.5	60	78	19.6	45.9	20.3 34
H5N1 Influenza virus [26]	1250	150	50	78	16.3	133.7	59.2 98.8
MS2 bacteriophage [27]	1100 1150	202.5	60	78	19.6	185.3	81.8 136.6
S. aureus bacteriophage [28]	2× mag 900	162	200	80	66.9	95.1	42 70.2

The grey shading average measured rather than a rated cavity-magnetron power.

recommendations to made in choice of a suitable microwave oven for MGS decontamination purposes. This approach can be applied in the assessment of future microwave oven designs for MGS decontamination processes, along with redesign rules of N95-like respirators that enables them to survive the MGS decontamination process.

6. Discussion

The paper has reviewed microwave *in-vitro* contact and non-contact detection of COVID-19, microwave disruption and inactivation of microorganisms (bacteria, fungi, and virus), and MGS decontamination of N95-like respirators. A discussion on these microwave processes now follows.

6.1. *In-Vitro* Microwave Rapid Detection of COVID-19

Proof of principle of *in-vitro* microwave rapid test measurements have been established, further work is required to define if the tests may be implemented in a blood bank within hospitals and health centers. As these tests require blood to be taken from the consenting patient, injection hesitancy [61] may prove to a prohibitive barrier if the tests are used to control travel at international airport, seaports, and land-boarders.

6.1.1. VNA Choice

Notwithstanding injection hesitancy, to enhance the probability of the uptake of these invasive tests, there is a need to demonstrate a predictive accuracy comparable to current molecular polymerase chain reaction and lateral flow tests, and at completive cost. With regard to cost, the choice of whether to use a portable/han-

dheld or bench top VNA is a significant factor, as many portable/handheld VNA have low dynamic range (typically 95 dB) and output power (typically 0 dBm) as compared to a bench top VNA that have a typical dynamic range of 125 dB and output power of 0 to 10 dBm. It is, therefore, important to compare directly the measurement resolution of different VNA's within future *in-vitro* rapid detection experiments.

6.1.2. Microwave Frequency Band Selection

There is now considerably evidence that healthily human blood and COVID-19 infected blood has microwave frequency dependency response away from the 2.45 GHz. Human blood relaxation measurements [39]-[46], swept frequency rapid detection experiments [8] [9], microwave feed-horn illumination experiments along with microorganism confined acoustic vibrations theory [31] [32] [33] [34] [35] indicate the frequency band of interest is between 8.0 to 10 s of GHz.

6.1.3. Contact or Non-Contact Antenna Design

The research into biosensors is a rapidly expanding field of interest. For microwave detection of COVID-19, the question whether contact or non-contact planar microstrip antenna provides the most detection sensitivity and selectivity is an important area of future research.

6.2. Mono-Mode Feed-Horn Inactivation of Microorganism

It is generally accepted that the microwave electric field energy couples to the dipole of polar molecules. Recently, it has been proposed that cytoplasm RNA (ribonucleic acid) within the virus spheroid volume collectively act as single dipole in the 8 GHz frequency range. Thereby allowing microwave energy to couple into the mechanical (acoustic) vibrational lowest mode ($l = 1$) [31] [32] [33] [34] [35]. This energy transfer phenomenon is termed Microwave Resonant Absorption (MRA) [30] [31], or Structure Resonance Energy Transfer (SRET) [33] [34] [35]. As this method of cell destruction becomes more widely accepted, longitudinal modes within rod-like shape viruses have also been examined in the 6 to 40 GHz range [34] [35]. Inherently, the mechanism assumes that an internal force displacement must overcome the rupture pressure of a solid boundary membrane, however further experimental and theoretical work is required to account for cell lysis [14] [16] [18]. A further feature of note is that MRA (SRET) closely resembles the simple theory of diocotron mode ($l = 1$) [62]: is association thereby provides additional investigation.

6.3. Microorganism Suspension Size, Geometry, and Location within Microwave Oven

Since the multi-mode microwave oven was first patented for treating food-stuff [63], it has been known that dielectric material (polar molecule, such as water and food-stuff), size, geometry, and location within the ovens cavity presents a number

of non-even heating challenges [64] [65]. It is standard practice that once heated; the food to be eaten should stand for a few minutes for conduction and convection processes to transmit heat throughout the food [66]. However, Geedipalli *et al.* [54] showed that food placed upon glass rotating carousel upon improved food temperature uniformity by 40%.

In 2002, Houšová and Hoke [67] studied the dielectric volume heating of small amounts of water (<250 ml) within four different domestic microwave ovens and found it to be oven-specific due to the oven's cavity size and position of the water load within the oven cavity. Above 250 ml of water, no dependence upon geometry of glass beaker and flat Petri dish could be derived for these domestic microwave ovens. An example of which is the Moulinex microwave oven; type FM 2915Q that has a rated power output 850 W, with a non-rotating glass shelf. They based their findings on Equation (4) [22] [37] [38] [53] [68] [69].

$$P_v = 2\pi f \varepsilon_0 \varepsilon'' |E|^2 \tag{4}$$

where P_v is power density in the load ($W \cdot m^{-3}$), the $2\pi f \varepsilon_0 \varepsilon''$ term represents the dielectric conductivity (σ) of the load, where f is the microwave frequency (2.45 GHz), ε_0 is the permittivity of free space (8.854×10^{-12} $F \cdot m^{-1}$), ε'' is the dielectric loss of the load, and E is the electric field strength inside the load ($V \cdot m^{-1}$) at the local position (x, y, z) within the multimode cavity. From this they calculated the relative absorbed power (P_a/P_{max}), where P_a is the amount of heated water, and P_{max} is the power absorbed by 1000 ml of water.

In this context the aliquots of microorganisms suspension reported in **Table 1** and **Table 2**; *i.e.*, 100 ml [13], 100 ml [14], 10 to 100 ml [15], 10 ml [16], and 50 ml [18] inactivation outcome is most likely to be oven-specific.

Given the theoretical maximum cavity unloaded Q-factor (Q_u) may be defined as in Equation (5) [52] [68].

$$Q_u = \frac{2V_c}{\delta A_c} \tag{5}$$

where V_c is the cavity volume, δ is the electrical skin depth of the cavity wall conductivity (typically 5 microns) and A_c is the cavity wall area. Thus, Q_u is defined as the ratio of stored energy in cavity to the energy loss to the cavity walls. Under load conditions the cavity Q-factor falls and is redefined as Q_l (Equation (6)) where V_l is the load volume.

$$Q_l = \frac{2(V_c - V_l)}{\delta A_c} \tag{6}$$

A worked example is given here. Introducing a small load volume ($V_l \sim 100$ ml (1×10^{-4} m^3) into the Moulinex oven (cavity volume = 0.0238 m^3, surface area = 0.5 m^2) reveals a Q-factor reduction from 19,040 to 18,960, or a 0.42% reduction. Under these load conditions, it is reasonable to assume that the ovens electric field pattern is not significantly altered and remains in a high Q mode where the electric field intensity alternates between high (hot-spots) and low (cool-spots) every ½ wavelength (~6.1 cm). This would indicate that the central

vertical axis of glass shelf were the load is placed experiences a hot-spot. Indeed multi-mode cavity, 3-dimensional (x, y, z) multiphysics models provide evidence for this assumption [53] [54] [69]. By extension, it is assumed that the medical syringe inactivation data reported in [15] [19] and towels [17] are comparable to each other and the flat Petre dish inactivation date.

6.4. Respirators Metal Noise Clips and Bubbles within a Microwave Oven

In some MGS decontamination studies it has been recorded that a metal nose-clip sometimes causes local burning damage in certain respirators models. It has been proposed that the mechanism for the burning damage is due to the metal noise clip acting like a microstrip operating in a quasi-transverse electromagnetic (TEM) mode [30]. Under these electromagnetic conditions and as the MGs decontamination proceeds with increasing temperature, the microstrip surrounding air is replaced by water vapor and ultimately steam causing the microstrip phase velocity to decreases with time. Thus the microstrip standing wave reduces in physical length resulting in short- and open-circuit nodes to momentarily align with protrusion and sharp edges of the metal nose clip causing high voltage stress points that lead to local heating and burning of the respirator polymer material.

6.5. Bubble Formation within a Microwave Oven

In this work the dielectric properties of the microorganism and suspension fluid are considered to have similar values at room temperature. However after a period of dielectric volume heating of the virus suspension the liquid-phase approaches saturation temperature, where bubble nucleation is promoted, and which grow in size, and then float to the free-surface where heat is lost from the bulk of the liquid-phase. As the bubbles grow in number a heterogeneous two-phase mixture develops, were the dissolved nature of the air bubbles alters the balk dielectric constant and is defined as (ε_m) where the subscript m is the liquid-bubble mixture. One way to calculate the binary mixture effective dielectric constant is to use a modified Looyenga cubic mixing formula [30] [53] [70] [71]. Equation (7) gives Looyenga's binary formula where the subscripts denote the liquid and gas vapor phase and a_g is the vapor fraction.

$$\varepsilon_m = \left[\left(\varepsilon_g^{1/3} - \varepsilon_l^{1/3}\right)\alpha_g + \varepsilon_l^{1/3}\right]^3 \tag{7}$$

For MGS decontamination of thermally sensitive N95-like respirators that begin to deform at temperatures close to 100˚C, it is worth noting that knowledge of bubble formation is beneficial as these bubbles should help to prevent superheating.

6.6. Non-Thermal and Thermal Microwave Oven Inactivation Mechanism

Microwave dielectric volume heating of polar molecules undergoes polarization and relaxations in their dipoles [36] [37] [64] [65] generating a faster mechanism

than thermal heat transfer due to conduction of heating from the outside of the vessel that hold the water. However, within the physical and engineering sciences is has been uncertainty if microwave irradiation alone can cause death in biological systems [72], whereas with more certainty thermal heating is known to cause microorganism inactivation > 50˚C [13]-[18] [53] [54] [55] [56] [58] [73] [74]. It is also known that inactivation of microorganism heterogeneous populations tend to follow a non-first-rate law [73] and microorganism homogeneous populations follow a first-order-rate law. In this work the inactivation of microorganism homogeneous populations has been reviewed and assumed to have a first-order-rate of inactivation, $[C] = [C_o]e^{-kt}$. Where $[C]$ is the reduction microorganism concentration, $[C_o]$ is the initial microorganism concentration, k is the rate constant, and t is time.

A comparison of thermal and non-thermal microwave disruption and inactivation (≥4 $\log_{10}$) of microorganisms is shown in **Figure 5**, where temperature is plotted on the horizontal axis and exposure time on the vertical axis. The microwave data is taken from **Tables 1-3**. In addition, thermal heat inactivation data is taken from [58] is also plotted. For the non-thermal microwave disruption studies, even though applied microwave power levels of 200 to 650 W are used, the dataset is in the low temperature range (20˚C to 29˚C). Whereas, the thermal microwave inactivation data is in the higher temperature range (50˚C to 86˚C) and is separated into two groups that are characterized by their applied

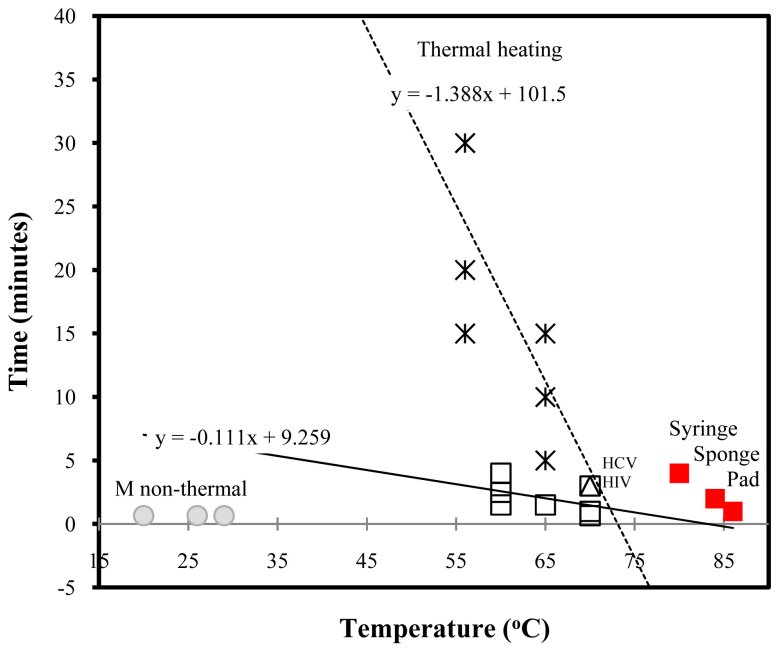

Figure 5. Thermal microwave, non-thermal microwave, and thermal treatment of microorganisms plotted as a function of time and temperature. The inactivation data point represents a ≥4 $\log_{10}$ reduction. *E coli* suspension; non-thermal microwave blue circles. *E. coli* thermal microwave (open squares) plus HCV and HIV (open triangle). *E. coli* soaked kitchen sponge and pad, and used syringe (red squares; 1.05 ± 0.050 kW). Thermal inactivation of SARS-CoV-2 suspension data (open stars with trend-line) is taken from [58].

microwave power (suspension fluid, syringe, and cigarette filters (100 to 650 W), and inoculated sponge, kitchen pad and syringe (1 to 1.1 kW)). The culture fluid suspension dataset, that includes HCV and HIV, has a 7-point trend-line of −1.1113 and temperature intercept of 74˚C. In comparison the soaked sponge, kitchen scouring pad, and used syringe dataset has a higher temperature intercept of 88˚C indicating a greater microorganism resilience on/in these fomites with respect to the liquid suspension. Note, the syringe requires 4 minutes for *E. coli* inactivation compared with the 1 and 2 minutes for kitchen sponge and kitchen pad. The thermal inactivation 8-point dataset trend-line is −1.3889, or approximately 12.5 times slower rate than the thermal microwave data, indicating a difference in inactivation mechanisms.

Figure 6 uses the same temperature x time domain as in Figure 5 to provide a comparison of thermal microwave inactivation (≥4 $\log_{10}$) of microorganism suspension, syringe, cigarette filter, plus inoculated N95-like respirators. The microwave data is taken from Table 1, Table 3 and Table 7. Here it is seen that the data point spatial spread is separated into three groups. That is, the *E. coli* suspension and HCV and HIV inoculated syringe, and cigarette filter at the lower 60˚C to 70˚C range with an associated power of 1 to 1.1 kW, Inoculated kitchen sponge, kitchen scouring pad and plastic syringe in the 80˚C to 90˚C and associated 1 to 1.1 kW, and the N95-like respirators temperature being defined by the boiling point of water (100˚C) at one atmospheric pressure with an associated power of 0.75 to 1.25 kW. It is concluded from this study that three temperature groups

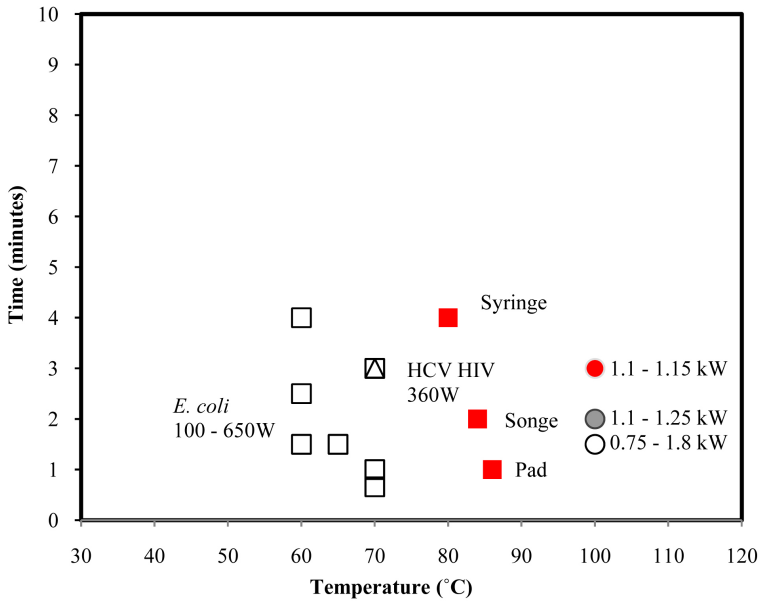

Figure 6. Thermal microwave inactivation (≥4 $\log_{10}$ reduction) of microorganisms plotted as a function of time and temperature. *E. coli* suspension; thermal microwave open squares circles. HCV and HIV suspension open square with triangle (360 W). *E. coli* inoculated sponge, kitchen pad, and syringe: red squares (1.05 ± 0.050 kW). MGS decontamination of N95-like respirators: open circle (0.75 and 1.8 kW), close blue circle (1.1 and 1.25 kW), and closed red circle (1.1 to 1.15 kW).

do not relate to the reported cavity-magnetron rate power and applied power. Indeed, the variance in the power groupings appears to be both oven-specific and fomite-specific.

Figure 7 provides an energy phase-space projection of process energy budget (kJ) on the horizontal-axis against the specific energy density of 1 ml of water liquid-phase (kJ·ml^{-1}) on the vertical-axis. Within the microorganism suspension dataset (beaker, sponge, scrubbing pads and MGS), thermodynamic analysis is used to provide further process clearly. In this projection least square trend-line can be fitted to the beaker, sponge, and MGS data points: starting from the vegetative bacteria and finishing with bacteria spores, with virus and their surrogates in the middle. As expected the bacteria spores are the most resilient to the thermal microwave irradiation stress. Using this knowledge, and as the trend-line progresses, the variance only increases around MGS decontamination points, indicating the possible presence of independent variables, such as respirator-type; water reservoir type (open water bath, bag or sterilizer), oven type (greatest variance is where 2 cavity-magnetrons are employed). Note that the beaker and sponge data points fit on a trend-line with an R^2 value of 0.896 indicting a strong association. With this analysis, it is reasonable to propose that the high degree of water absorption and retention (approximately 90% by volume) within the soaked sponge volume behaves like the beaker microorganism suspensions where the suspension

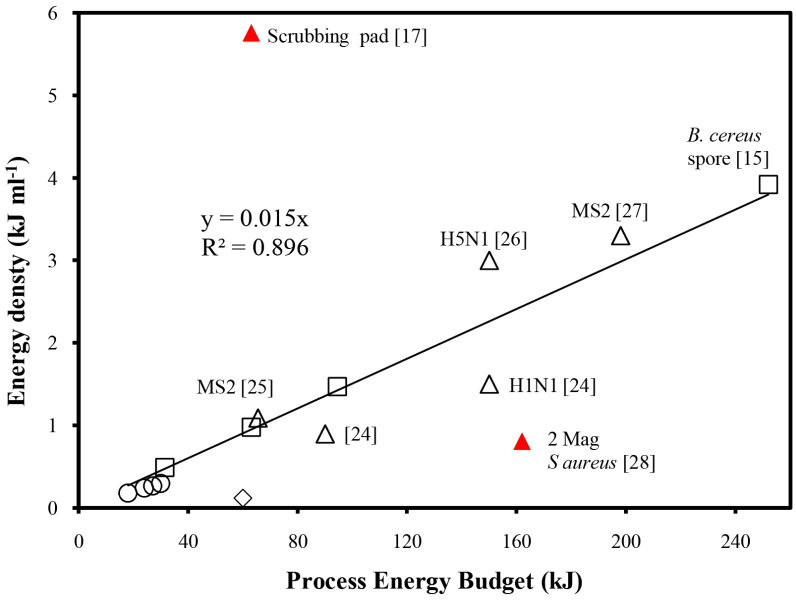

Figure 7. The microwave inactivation (≥4 $\log_{10}$) data presented in Figure 5 and Figure 6, is now presented using a thermodynamic analyses approach, were the process energy budget is plotted against specific energy density of liquid suspension (kJ·ml^{-1}). *E. coli* beaker; open circles (100 to 300 W [13]). *E. coli* and *B. subtitles* beaker; open diamond (600 W [14]). *E. coli*, MS2, *B. cereus* and *B. cereus* spores inoculated sponge; open squares (1.05 ± 0.050 kW [15]). *E. coli* inoculated kitchen scrubbing pad: open squares (1.05 ± 0.050 kW CW [15]). MGS decontamination of N95-like respirators using: open triangles (0.75 to 1.8 kW [23]-[28]). Least square tend-line excludes the two outliers (red filled square and triangle).

is retained by means of beaker containing wall. Finally there does not appear to be a duty cycle dependency which would suggest that cell wall disruption is masked by the thermal microwave irradiation.

As regards to the outliers: the scrubbing pad (red square) is excluded from the trend-line due to its poor water and absorption and retention properties (approximately 26% by volume), in addition the 2 cavity-magnetron data point (red triangle) is excluded due to the high rated power used (1800 W) and the bi-directional applied power (top and bottom) [30]. Not shown in **Figure 7** is the 1 to 10 ml of microorganism suspension used to inoculate towels [17], syringes and cigarette filters [15] [19], due to the inevitable outcome being a relative and disproportionate high energy density value, compared to the beaker, sponge and MGS outcomes. This is because the low volumes used were intended to simulate real-life health care environments and within populations of PWID: where a relative high fraction of the fomite (glass, plastic, or gauze) undergoing dielectric volume heating.

The use of Looyenga's heterogeneous binary formula may assist in the understanding of microwave sterilization of used syringes [15] [19] and used towels [17], where the volume (mass) fraction of suspension liquid (a_l) is smaller than both the fomite volume and mass. This aspect of Looyenya's formula may be used as an exclusion criterion, where the fomite fraction is likely to be 95% to 99%. For this reason, the inactivation (≥4 $\log_{10}$) data obtained for: used towels, scrubbing pads, syringes, and cigarette filters are collected separately and presented in **Table 8** that includes an estimation of suspension plus the unknown additional water content for the moist towel. Notwithstanding the lack of moisture content knowledge within the towel, the available data shows that the empty used syringe provides the highest process energy budget. This limited data suggests the near-empty plastic syringe has a low rate of microwave energy absorption compared to the other fomites containing water. From a HCV and HIV infection prevention perspective, it would appear that placing the contaminated near-empty syringes in an open water bath prior to microwave treatment; thereby help standardized sterilization protocols within PWID populations.

Table 8. Inactivation (≥4 $\log_{10}$) data obtained for used: towel, scrubbing pad, syringe, and cigarette filter.

Fomite—microorganism [reference]	Power (W)	Time (t)	Process energy budget (kJ)	Suspension (moisture content plus water)
Moist towel—*S. aureus, P. aeruginos* and *C. albicans [17]*	500	120	60	1 ml (moisture? +50 ml)
Scrubbing pad—*E. coli* [15]	1050	60	63	10.94 ml
Used plastic syringe—*E. coli* [15]	1050	240	252	empty
Insulin syringe—HCV [19]	360	180	64.8	40 ml
Insulin syringe—HIV [19]	360	180	64.8	40.ml
Cigarette filter—HCV [19]	360	180	64.8	>0.5 ml [59]
Cigarette filter—HIV [19]	360	180	64.8	>0.5 ml [59]

7. Summary and Outlook

This paper has reviewed three interactions between microwave energy and microorganisms (bacteria, fungi, and viruses). The interactions are characterized by their electrical power, mode of power delivery (mono-mode 50-Ohm transmission-line, the feed-horn illumination, and multimode microwave oven), and microorganism outcome (*in-vitro* contaminated human blood detection, cell-wall disruption, and inactivation). In the latter case, the purpose of inactivation was not only to kill the virus, but also to re-use the decontaminated fomite (HCV and HIV contaminated syringe and cigarette filter, and influenza virus contaminated N95-like respirator). For this dual requirement, the applied energy in the form of dielectric volume heating needs be to sufficient to kill the virus but not sufficient to damage the fomite.

Given these requirements, the three microwave energy processes relate to the following. For *in-vitro* virus-contaminated blood detection: 0 to 10 dBm @ 2 to 8.5 GHz; for feed-horn illumination and inactivation: 1 to 6.5 W @ 8 to 26 GHz at the feed-horn illumination an applied power density of 10 to 100 mW^{-2} at the virus suffice. The third energy process that is within a multi-mode microwave oven uses 100 s of W @ 300 to 1800 W @ 2.45 GHz for inactivation, with temperature control between 70˚C to 100˚C for reuse purposes.

Mechanisms for the three microwave interactions are also discussed. Swept frequency analysis of transmission-line terminated with a non-50-Ohm virus load, chemical cellular lysis, and microwave resonant absorption causing cell wall rupture. In addition, the examination of the thermodynamics of input and output process energy budget has been performed with the aim of revealing the inactivation mechanisms in different microorganism suspension volumes and the inactivation of microorganisms on and within different fomites (kitchen sponge, scouring pads syringes cigarette filters and N95-like respirators). To this end, the size of microorganism suspension, geometry, and location within microwave oven have been discussed. Looyena's heterogeneous binary mixture formula may help in the understanding of how fomites influence the microwave inactivation outcome.

The overall conclusion from this study is that the mechanism of microwave interaction with microorganisms is complex and is clearly dependent on the microorganism type, along with the treatment time and the level of energy imparted by the microwave source. As regards the outlook of the work, there are many research questions that remain to be investigated, two of which are listed here.

1) In the case of the microwave swept frequency of healthy and infected blood studies, it would useful to undertake a lumped (inductor, capacitor, and resister) linear circuit analysis [49] [50] of the non-biological components (transmission-line and test chamber) and compare them to the physiochemical components of the healthy and infected blood. Here is hoped that the LCR elements may provide and insight into the shape and depth of the zeros.

2) The reduced information within the energy phase-space projection of the multi-mode microwave oven inactivation data provides a degree of clarity in the microorganism inactivation process. Here it may useful to use multi-variant tools, such as principal component analysis [75], to differentiate further between the independent variables (number of cavity-magnetrons used and the direction of illumination, fomite, and microorganism). The score information could then be used to standardize future multi-mode microwave oven studies.

Conflicts of Interest

The authors declare they have no conflicts of interest.

References

[1] Wells, H.G. (1898) The Time Machine. 1st Edition, William Heinemann, London.

[2] Wells, H.G. (1898) War of the Worlds Novel. 1st Edition, William Heinemann, London.

[3] Luk, J., Gross, P. and Thompson, W.W. (2001) Observations on Mortality during the 1918 Influenza Pandemic. *Clinical Infectious Diseases*, **33**, 1375-1378. https://doi.org/10.1086/322662

[4] Samanlioglu, F. and Bilge, A.H. (2016) An Overview of the 2009 A(H1N1) Pandemic in Europe: Efficiency of the Vaccination and Healthcare Strategies. *Journal of Healthcare Engineering*, **2016**, Article ID: 5965836. https://doi.org/10.1155/2016/5965836

[5] Watkins, J. (2020) Preventing a Covid-19 Pandemic. *BMJ*, **368**, m810. https://doi.org/10.1136/bmj.m810

[6] Hassan, F., London, L. and Gonsalves, G. (2021) Unequal Global Vaccine Coverage Is at the Heart of the Current Covid-19 Crisis. *BMJ*, **375**, n3074. https://doi.org/10.1136/bmj.n3074

[7] Silva, A.L.P., Prata, J.C., Walker, T.R., Duarte, A.C., Ouyang, W., Barcelò D. and Rocha-Santos, T. (2021) Increased Plastic Pollution Due to COVID-19 Pandemic: Challenges and Recommendations. *Chemical Engineering Journal*, **405**, Article ID: 126683. https://doi.org/10.1016/j.cej.2020.126683

[8] Abdulkarim, Y.I., Awl, H.N., Muhammadsharif, F.F., Sidiq, K.R., Saeed, S.R., Karaaslan, M., Huang, S., Luo, H. and Deng, L. (2020) Design and Study of a Coronavirus-Shaped Metamaterial Sensor Stimulated by Electromagnetic Waves for Rapid Diagnosis of Covid-19. arXiv Preprint arXiv:2009.08862.

[9] Elsheakh, D.M., Ahmed, M.I., Elashry, G.M., Moghannem, S.M., Elsadek, H.A., Elmazny, W.N., Alieldin, N.H. and Abdallah, E.A. (2021) Rapid Detection of Coronavirus (COVID-19) Using Microwave Immunosensor Cavity Resonator. *Sensors*, **21**, Article No. 7021. https://doi.org/10.3390/s21217021

[10] Jofre, M., Jofre, L. and Jofre-Roca, L. (2021) On the Wireless Microwave Sensing of Bacterial Membrane Potential in Microfluidic-Actuated Platforms. *Sensors*, **21**, Article No. 2420. https://doi.org/10.3390/s21103420

[11] Akter, N., Hasan, M.M and Pala, N. (2021) A Review of THz Technologies for Rapid Sensing and Detection of Viruses Including SARS-CoV-2. *Biosensors*, **11**, Article No. 349. https://doi.org/10.3390/bios11100349

[12] Abo-Seidaa, O.M., Eldabe, N.T.M., Abu-Shady, M. and Ali, A.R. (2021) The Effect of

Nanoparticles and Electromagnetic Waves on Coronavirus (COVID-19) Using a Rectangular Waveguide Cavity Resonator. ResearchGate. https://www.researchgate https://www.researchgate.net/profile/Osama-Abo-Seida

[13] Fujikawa, H., Ushioda, H. and Kudo, Y. (1992) Kinetics of *Escherichia coli* Destruction by Microwave Irradiation. *Applied and Environmental Microbiology*, **58**, 920-924. https://doi.org/10.1128/aem.58.3.920-924.1992

[14] Woo, I.S., Rhee, I.K. and Park, H.D. (2000) Differential Damage in Bacterial Cells by Microwave Radiation on the Basis of Cell Wall Structure. *Applied and Environmental Microbiology*, **66**, 2243-2247. https://doi.org/10.1128/AEM.66.5.2243-2247.2000

[15] Park, D.K., Bitton, G. and Melker, R. (2006) Microbial Inactivation by Microwave Radiation in the Home Environment. *Journal of Environmental Health*, **69**, 17-24.

[16] Asay, B., Tebaykina, Z., Vlasova, A. and Wen, M. (2008) Membrane Composition as a Factor in Susceptibility of *Escherichia coli* C29 to Thermal and Non-Thermal Microwave Radiation. *Journal of Experimental Microbiology and Immunology*, **12**, 7-13.

[17] Tanaka, Y., Fujiwara, S., Kataoka, D., Takagaki, T., Takano, S., Honda, S., Katayose, M., Kinosita, Y. and Toyoshima, Y. (1998) Warming and Sterilizing Towels by Microwave Irradiation. *Yonago Acta Medica*, **41**, 83-88.

[18] Barnett, C., Huerta-Mounoz, U., James, R. and Pauls, G. (2006) The Use of Microwave Radiation in Combination with EDTA as an Outer Membrane Disruption Technique to Preserve Metalloenzyme Activity in *Escherichia coli*. *Journal of Experimental Microbiology and Immunology*, **9**, 1-5.

[19] Siddharta, A., Pfaender, S., Malassa, A., Doerrbecker, J., Anggakusuma, Engelmann, M., Nugraha, B., *et al.* (2016) Inactivation of HCV and HIV by Microwave: A Novel Approach for Prevention of Virus Transmission among People Who Inject Drugs. *Scientific Reports*, **6**, Article No. 36619. https://doi.org/10.1038/srep36619

[20] Wu, Y. and Yao, M. (2010) Inactivation of Bacteria and Fungus Aerosols Using Microwave Irradiation. *Journal of Aerosol Science*, **41**, 682-693. https://doi.org/10.1016/j.jaerosci.2010.04.004

[21] Wu, Y. and Yao, M. (2014) *In Situ* Airborne Virus Inactivation by Microwave Irradiation. *Chinese Science Bulletin*, **59**, 1438-1445. https://doi.org/10.1007/s11434-014-0171-3

[22] Wang, C., Hua, X. and Zhanga, Z. (2019) Airborne Disinfection Using Microwave-Based Technology: Energy Efficient and Distinct Inactivation Mechanism Compared with Waterborne Disinfection. *Journal of Aerosol Science*, **137**, Article ID: 105437. https://doi.org/10.1016/j.jaerosci.2019.105437

[23] Bergman, M.S., Viscusi, D.J., Heimbuch, B.K., Wander, J.D., Sambol, A.R. and Shaffer, R.E. (2010) Evaluation of Multiple (3-Cycle) Decontamination Processing for Filtering Facepiece Respirators. *Journal of Engineered Fibers and Fabrics*, **5**, 33-41. https://doi.org/10.1177/155892501000500405

[24] Heimbuch, B.K., Wallace, W.H., Kinney, K.R., Lumley, A.E., Wu, C.-Y., Wo, M.-H. and Wander, J.D. (2011) A Pandemic Influenza Preparedness Study: Use of Energetic Methods to Decontaminate Filtering Facepiece Respirators Contaminated with H1N1 Aerosols and Droplets. *American Journal of Infection Control*, **39**, e1-e9. https://doi.org/10.1016/j.ajic.2010.07.004

[25] Fisher, E.M., Williams, J.L. and Shaffer, R. (2011) Evaluation of Microwave Steam Bags for the Decontamination of Filtering Facepiece Respirators. *PLoS ONE*, **6**, Article ID: e18585. https://doi.org/10.1371/journal.pone.0018585

[26] Lore, M.B., Heimbuch, B.K., Brown, T.L., Wander, J.D. and Hinrichs, S.H. (2012) Effectiveness of Three Decontamination Treatments against Influenza Virus Applied to Filtering Facepiece Respirators. *Annals of Occupational Hygiene*, **56**, 92-101.

[27] Zulauf, K.E., Green, A.B., Ba, A.N.N., Jagdish, T., Reif, D., Seeley, R., Dale, A. and Kirby, J.E. (2020) Microwave-Generated Steam Decontamination of N95 Respirators Utilizing Universally Accessible Materials. *mBio*, **11**, Article ID: e00997. https://doi.org/10.1128/mBio.00997-20

[28] Pascoe, M.J., Robertson, A., Crayford, A., Durand, E., Steer, J., Castelli, A., Wesgate, R., Evans, S.L., Porch, A. and Maillard, J.-Y. (2020) Dry Heat and Microwave-Generated Steam Protocols for the Rapid Decontamination of Respiratory Personal Protective Equipment in Response to COVID-19-Related Shortages. *Journal of Hospital Infection*, **106**, 10-19. https://doi.org/10.1016/j.jhin.2020.07.008

[29] Law, V.J. and Dowling, D.P. (2021) MGS Decontamination of Respirators: A Thermodynamic Analysis. *Global Journal of Research in Engineering & Computer Sciences*, **1**, 1-17.

[30] Law, V.J. and Dowling, D.P. (2021) MGS Decontamination of Respirators: Dielectric Considerations. *Global Journal of Research in Engineering & Computer Sciences*, **1**, 6-21.

[31] Liu, T.M., Chen, H.-P., Wang, L.-T., Wang, J.-R., Luo, T.-N., Chen, Y.-J., *et al.* (2009) Microwave Resonant Absorption of Viruses through Dipolar Coupling with Confined Acoustic Vibrations. *Applied Physics Letters*, **94**, Article ID: 043902. https://doi.org/10.1063/1.3074371

[32] Hung, W.T., Tung, J.-J. and Chen, S.Y. (2014) A Focusing Reflectarray and Its Application in Microwave Virus Sanitizer. *Radio Science*, **49**, 890-898. https://doi.org/10.1002/2014RS005481

[33] Yang, S.C., Lin, H.C., Liu, T.M., Lu, J.T., Hung, W.T., Huang, Y.R., *et al.* (2015) Efficient Structure Resonance Energy Transfer from Microwaves to Confined Acoustic Vibrations in Viruses. *Scientific Reports*, **5**, Article No.18030. https://doi.org/10.1038/srep18030

[34] Sun, C.K., Tsail, Y.C., Chen, Y.J.E., Liu, T.M., Chen, H.Y., Wang, H.C. and Lo, C.F. (2017) Resonant Dipolar Coupling of Microwaves with Confined Acoustic Vibrations in a Rod-Shaped Virus. *Scientific Reports*, **7**, Article No. 4611. https://doi.org/10.1038/s41598-017-04089-7

[35] Sun, C.K. and Liu, T.M. (2011) Microwave Resonant Absorption Method and Device for Viruses Inactivation. US Patent No. US20110070624A1.

[36] Perreux, L. and Loupy, A. (2001) A Tentative Rationalization of Microwave Effects in Organic Synthesis According to Reaction Medium and Mechanism Considerations. *Tetrahedron*, **57**, 9199-9223. https://doi.org/10.1016/S0040-4020(01)00905-X

[37] Sun, J., Wang, W. and Yue, Q. (2016) Review on Microwave-Matter Interaction Fundamentals and Efficient Microwave-Associated Heating Strategies. *Materials*, **9**, Article No. 231. https://doi.org/10.3390/ma9040231

[38] Law, V.J. and Denis, D.P. (2018) Domestic Microwave Oven and Fixed Geometry Waveguide Applicator Processing of Organic Compounds and Biomaterials: A Review. *Global Journal of Researches in Engineering*: *A Mechanical and Mechanics Engineering*, **S1**.

[39] Malmberg, C.G. and Maryott, A.A. (1956) Dielectric Constant of Water from 0˚ to 100˚C. *Journal of Research of the National Bureau of Standards*, **56**, Article No. 2641.

[40] Cook, H.F. (1951) Dielectric Behaviour of Human Blood at Microwave Frequencies. *Nature*, **168**, 247-248. https://doi.org/10.1038/168247a0

[41] Cook, H.F. (1952) A Comparison of the Dielectric Behavior of Pure Water and Human Blood at Microwave Frequencies. *British Journal of Applied Physics*, **3**, 249-255. https://doi.org/10.1088/0508-3443/3/8/302

[42] Wolf, M., Gulich, R., Lunkenheimer, P. and Loidl, A. (2011) Broadband Dielectric Spectroscopy on Human Blood. *Biochimica et Biophysica Acta* (*BBA*)—*General Subjects*, **1810**, 727-740. https://doi.org/10.1016/j.bbagen.2011.05.012

[43] Abdalla, S. (2011) Gaussian Distribution of Relaxation through Human Blood. *Physica B*, **406**, 584-587. https://doi.org/10.1016/j.physb.2010.11.047

[44] Farsaci, F., Ficarra, S., Russo, A., Galtieri, A. and Tellone, E. (2015) Dielectric Properties of Human Diabetic Blood: Thermodynamic Characterization and New Prospective for Alternative Diagnostic Techniques. *Journal of Advance Dielectrics*, **5**, Article ID: 1550021. https://doi.org/10.1142/S2010135X15500216

[45] Sodhi, C.S., de Sena, L.C., Ozelim, M. and Rathie, P.N. (2021) Dielectric Relaxation Model of Human Blood as a Superposition of Debye Functions with Relaxation Times Following a Modified-Weibull Distribution. *Heliyon*, **7**, Article ID: e06606. https://doi.org/10.1016/j.heliyon.2021.e06606

[46] Salahuddin, S., Farrugia, L., Sammut, C.V., O'Halloran, M. and Porter, E. (2007) Dielectric Properties of Fresh Human Blood. 2007 *International Conference on Electromagnetic in Advanced Applications*, Verona, 11-15 September 2017, 356-359. https://doi.org/10.1109/ICEAA.2017.8065249

[47] Han, Q., Wen, X., Wang, L., Han, X., Shen, Y., Cao, J., *et al.* (2020) Role of Hematological Parameters in the Diagnosis of Influenza Virus Infection in Patients with Respiratory Tract Infection Symptoms. *Journal of Clinical Laboratory Analysis*, **34**, Article ID: e23191. https://doi.org/10.1002/jcla.23191

[48] Lei, J., Li, J., Li, X. and Qi, X. (2020) CT Imaging of the 2019 Novel Coronavirus (2019-nCoV) Pneumonia. *Radiology*, **295**, 18 p. https://doi.org/10.1148/radiol.2020200236

[49] Law, V.J. (2008) Non-Invasive VHF Injected Signal Monitoring in Atmospheric Pressure Plasma and Axial DC Magnetron. *Vacuum*, **82**, 514-520. https://doi.org/10.1016/j.vacuum.2007.08.007

[50] Law, V.J., Lawler, J. and Daniels, S. (2008) Process-Induced Oscillator Frequency Pulling and Phase Noise within Plasma Systems. *Vacuum*, **82**, 630-638. https://doi.org/10.1016/j.vacuum.2007.10.001

[51] (2011) Industrial Microwave Heating Installations. Test Methods for the Determination of Power Output. CSN EN 61307 ed. 3.

[52] Law, V.J. and Dowling, D.P. (2019) Microwave oven Plasma Reactor Moding and Its Detection. 12*th Chaotic Modeling and Simulation International Conference*, Crete, 18-22 June, 157-179. https://doi.org/10.1007/978-3-030-39515-5_14

[53] Lee, G.L., Law, M.C. and Lee, V.C.C. (2020) Numerical Modelling of Liquid Heating and Boiling Phenomena under Microwave Irradiation Using OpenFOAM. *International Journal of Heat and Mass Transfer*, **148**, Article ID: 119096. https://doi.org/10.1016/j.ijheatmasstransfer.2019.119096

[54] Geedipalli, S.S.R., Rakesh, V. and Datta, A.K. (2007) Modeling the Heating Uniformity Contributed by a Rotating Turntable in Microwave Ovens. *Journal of Food Engineering*, **82**, 359-368. https://doi.org/10.1016/j.jfoodeng.2007.02.050

[55] Hayes, B.L. (2004) Recent Advances in Microwave-Assisted Synthesis. *Aldrichimica Acta*, **17**, 66-76.

[56] Hayes, B.L. and Collins, M.J. (2005) Reaction and Temperature Control for High Power Microwave-Assisted Chemistry Techniques. United States Patent No. US6917023B2.

[57] Law, V.J. and Dowling, D.P. (2018) The Domestic Microwave Oven as a Rapid Prototyping Tool. *Analytical Chemistry*: *An Indian Journal*, **18**, Article No. 139.

[58] Abraham, J.P., Plourde, B.D. and Cheng, L. (2020) Using Heat to Kill SARS-CoV-2. *Reviews in Medical Virology*, **30**, Article ID: e2115. https://doi.org/10.1002/rmv.2115

[59] Wahi, A. (2009) Scouring Pad. Patent No. US20090106920A1.

[60] Register, K.M. (2000) Underwater Naturalist. *Bulletin of the American Littoral Society*, **25**, 23-29.

[61] Freeman, D., Lambe, S., Yu, L., Freeman, J., Chadwick, A., Vaccari, C., *et al.* (2021) Injection Fears and COVID-19 Vaccine Hesitancy. *Psychological Medicine*, 1-11. https://doi.org/10.1017/S0033291721002609

[62] Fine, K.S. (1992) Simple Theory of a Nonlinear Diocotron Mode. *Physics of Fluids B: Plasma Physics*, **4**, 3981-3984. https://doi.org/10.1063/1.860301

[63] Spencer, P.L. (1950) Method of Treating Foodstuffs. Patent No. US2495429A.

[64] Gedye, R.N., Smith, F. and Westaway, K.C. (1988) The Rapid Synthesis of Organic Compounds in Microwave Ovens. *Canadian Journal Chemistry*, **66**, 17-26. https://doi.org/10.1139/v88-003

[65] Gedye, R.N., Rank, W. and Westaway, K.C. (1991) The Rapid Synthesis of Organic Compounds in Microwave Ovens. II. *Canadian Journal Chemistry*, **69**, 706-711. https://doi.org/10.1139/v91-106

[66] Ahmed, J. and Ramasamy, H.S. (2007) Chapter 28. Microwave Pasteurization and Sterilization of Foods. In: Rahman, S., Ed., *Handbook of Food Preservation*, Second Edition, CRC Press, Boca Raton, 709-730.

[67] Houšová, J. and Hoke, K. (2002) Microwave Heating—The Influence of Oven and Load Parameters on the Power Absorbed in the Heated Load. *Czech Journal of Food Sciences*, **20**, 117-124. https://doi.org/10.17221/3521-CJFS

[68] Law, V.J. (1998) Microwave Near-Field Plasma Probe. *Vacuum*, **51**, 463-468. https://doi.org/10.1016/S0042-207X(98)00199-7

[69] Yeong, S.P., Law, M.C., Lee, V.C.C. and Chan, Y.S. (2017) Modelling Batch Microwave Heating of Water. *IOP Conference Series: Materials Science and Engineering*, **217**, Article ID: 012035. https://doi.org/10.1088/1757-899X/217/1/012035

[70] Looyenga, H. (1965) Dielectric Constants of Heterogeneous Mixtures. *Physica*, **31**, 401-406. https://doi.org/10.1016/0031-8914(65)90045-5

[71] Anguelova, M.D. (2008) Complex Dielectric Constant of Sea Foam at Microwave Frequencies. *Journal of Geophysical Research*, **113**, Article No. C08001. https://doi.org/10.1029/2007JC004212

[72] Rougier, C., Prorot, A., Chazal, P., Leveque, P. and Lepratb, P. (2014) Thermal and Non-thermal Effects of Discontinuous Microwave Exposure (2.45 Gigahertz) on the Cell Membrane of *Escherichia coli*. *Applied and Environmental Microbiology*, **80**, 4832-4841. https://doi.org/10.1128/AEM.00789-14

[73] Yap, T.F., Liu, Z., Shveda, R.A. and Preston, D.J. (2020) A Predictive Model of the Temperature-Dependent Inactivation of Coronaviruses. *Applied Physics Letters*, **117**, Article ID: 060601. https://doi.org/10.1063/5.0020782

[74] Kampf, G., Todt, D., Pfaender, S. and Steinmann, E. (2020) Persistence of Coronaviruses on Inanimate Surfaces and Their Inactivation with Biocidal Agents. *Journal of Hospital Infection*, **104**, 246-251. https://doi.org/10.1016/j.jhin.2020.01.022

[75] Law, V.J., O'Connor, N., Twomey, B. Dowling, D.P. and Daniels, S. (2009) Visualization of Atmospheric Pressure Plasma Electrical Parameters. In: Skiadas, C.H., Dimotikalis, I. and Skiadas, C., Eds., *Topics on Chaotic Systems: Selected Papers from Chaos* 2008 *International Conference*, World Scientific, Singapore, 204-213. https://doi.org/10.1142/9789814271349_0024